Proteomics Analysis of Extracellular Matrix Remodeling During Zebrafish Heart Regeneration

Authors

Anna Garcia-Puig, Jose Luis Mosquera, Senda Jiménez-Delgado, Cristina García-Pastor, Ignasi Jorba, Daniel Navajas, Francesc Canals, and Angel Raya

Correspondence

araya@cmrb.eu

In Brief

Zebrafish can regenerate their hearts. The role of the extracellular matrix in this process is largely unknown. We have analyzed the proteome in control hearts and at different times of regeneration. Decellularization of samples allowed for enrichment of extracellular matrix proteins, increasing their detection. The results reported dynamic changes in specific proteins associated with specific stages of the regenerative process. Biomechanical analysis by atomic force microscopy revealed concomitant changes in matrix stiffness during this process.

Graphical Abstract

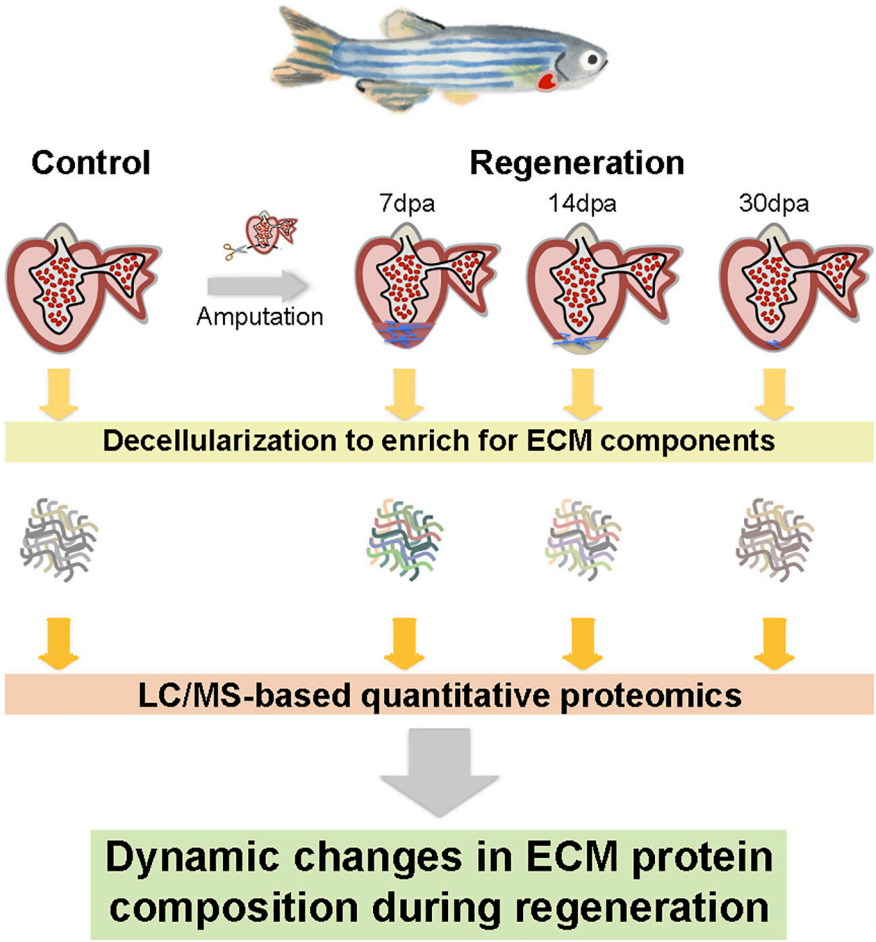

Highlights

- We have developed a decellularization protocol for ECM protein enrichment.
- We have characterized the proteome of adult zebrafish heart ECM.
- We describe dynamic changes in heart ECM proteome during regeneration.
- We describe changes in heart ECM stiffness during regeneration.

Garcia-Puig et al., 2019, Molecular & Cellular Proteomics *18*, 1745–1755

https://doi.org/10.1074/mcp.RA118.001193

⌘ *Author's Choice*

Proteomics Analysis of Extracellular Matrix Remodeling During Zebrafish Heart Regeneration*[S]

Anna Garcia-Puig‡§, Jose Luis Mosquera¶, Senda Jiménez-Delgado‡, Cristina García-Pastor‡, Ignasi Jorba‖‡‡, Daniel Navajas‖**‡‡, Francesc Canals§§, and Angel Raya‡§¶¶‖‖**

Adult zebrafish, in contrast to mammals, are able to regenerate their hearts in response to injury or experimental amputation. Our understanding of the cellular and molecular bases that underlie this process, although fragmentary, has increased significantly over the last years. However, the role of the extracellular matrix (ECM) during zebrafish heart regeneration has been comparatively rarely explored. Here, we set out to characterize the ECM protein composition in adult zebrafish hearts, and whether it changed during the regenerative response. For this purpose, we first established a decellularization protocol of adult zebrafish ventricles that significantly enriched the yield of ECM proteins. We then performed proteomic analyses of decellularized control hearts and at different times of regeneration. Our results show a dynamic change in ECM protein composition, most evident at the earliest (7 days postamputation) time point analyzed. Regeneration associated with sharp increases in specific ECM proteins, and with an overall decrease in collagens and cytoskeletal proteins. We finally tested by atomic force microscopy that the changes in ECM composition translated to decreased ECM stiffness. Our cumulative results identify changes in the protein composition and mechanical properties of the zebrafish heart ECM during regeneration. ***Molecular & Cellular Proteomics 18: 1745–1755, 2019. DOI: 10.1074/mcp.RA118.001193.***

According to the World Health Organization, 1/3 of all global deaths are because of cardiovascular diseases (1), which makes them the leading cause of morbidity and mortality among humans (2). This is generally thought to be the consequence of the limited capacity of the adult mammalian heart to recover after injury. Although some studies have reported that mammalian cardiomyocytes can experience limited proliferation after cellular damage, this is not enough to completely recover the lost tissue (3–5). After a lesion, the damaged cardiac tissue is replaced by a fibrotic scar, which reduces heart performance and may eventually lead to heart failure (6, 7).

Regeneration is a process by which organisms restore organs or tissues lost to injury or experimental amputation. This complex process gives rise to a tissue or organ nearly identical to the undamaged one. The understanding of regenerative processes is expected to help designing regenerative medicine strategies to address a variety of diseases. Even though neonatal mice have been shown to regenerate their hearts after an injury (8–13), the par excellence regenerative organisms are nonmammalian vertebrates such as urodele amphibians and zebrafish (14–17). Zebrafish can regenerate their heart after a 20% amputation (18, 19), cryoinjury (20–23) or genetic ablation (24). It has been demonstrated that this process occurs by limited dedifferentiation and proliferation of cardiomyocytes through the expression of cell-cycle regulators such as *plk1* and *mps1*, or chromatin-remodeling factors such as *brg1* (18, 25). Not only cardiomyocyte proliferation is essential for cardiac regeneration, but also cell migration, with cardiomyocytes near to the damaged tissue contributing to the regenerated tissue (26, 27). Moreover, epicardium activation and migration are also required for the completion of the process (28–30). In contrast with our understanding of the

From the ‡Center of Regenerative Medicine in Barcelona (CMRB), ¶Bioinformatics Unit, Institut d'Investigació Biomè dica de Bellvitge IDIBELL), 3rd Floor Hospital Duran i Reynals, Avinguda de la Gran Via 199-203, 08908 Hospitalet de Llobregat, Barcelona, Spain; §Center for Networked Biomedical Research on Bioengineering, Biomaterials and Nanomedicine (CIBER-BBN), 08908 Hospitalet de Llobregat (Barcelona), Spain; ‖Institute for Bioengineering of Catalonia (IBEC), Barcelona Science Park, Baldiri Reixac 15-21, 08028 Barcelona, Spain; **Unit of Biophysics and Bioengineering, Department of Physiological Sciences I, School of Medicine, University of Barcelona, Casanova 143, 08036 Barcelona, Spain; ‡‡Center for Networked Biomedical Research on Respiratory Diseases (CIBERES), 08036 Barcelona, Spain; §§Proteomics group, Vall d'Hebron Institut of Oncology (VHIO), Cellex center, Natzaret 115-117, 08035 Barcelona, Spain; ¶¶Institució Catalana de Recerca i Estudis Avançats (ICREA), 08010 Barcelona, Spain

Received November 20, 2018, and in revised form, June 3, 2019
Published, MCP Papers in Press, June 20, 2019, DOI 10.1074/mcp.RA118.001193

cellular bases underlying zebrafish heart regeneration, the role of the extracellular matrix (ECM)[1] in this process has received little attention (31–33).

Collagens, proteoglycans and glycoproteins form a complex structure, the ECM, which provides structural and mechanical support to tissues. In addition to a structural role, the ECM also instructs neighboring cells through biochemical and biomechanical signals that result in distinct biological responses (34, 35). Indeed, the composition and mechanical properties of the ECM play crucial roles determining cell behaviors such as proliferation, migration, differentiation, and apoptosis (36, 37). ECM remodeling is important during development, wound healing and disease states like cancer (36, 38–41). Studies using artificial ECM scaffolds have showed that physical properties of the ECM such as pore size, stiffness, fiber diameter, and chemical crosslinking also have effects on cell fate (42, 43). For instance, substrate stiffness induced myoskeleton reorganization, thus determining the cell shape of rat and mice neonatal cardiomyocytes, whereas dedifferentiation of neonatal cardiomyocytes and enhanced proliferation occurred in compliant matrices (43).

The role of the ECM during zebrafish heart regeneration has received little attention thus far. Gene expression analysis performed in regenerating hearts identified transcripts encoding ECM-related proteins among the most differentially expressed during this process (44–46). These included inhibitors of metalloproteinases, matrix metalloproteinases, and tenascin C (tnc), *tnc* transcripts being found overexpressed in the border zone between the healthy myocardium and the injury site (21, 47). Another study showed that fibronectin (fn) synthesis by epicardial cells was essential for zebrafish heart regeneration, probably by providing cues for cardiomyocyte migration (31). A role of hyaluronic acid (HA) signaling during zebrafish heart regeneration has also been proposed, because components of this pathway were found expressed in response to injury, and blocking HA signaling impaired regeneration (32). These three ECM components (tnc, fn, and HA) have been shown to form a pro-regenerative matrix in newt heart (48). Thus, a comprehensive study of the zebrafish heart ECM composition and characteristics may reveal other key points in the heart regeneration process. In the present study, we have developed a protocol to decellularize adult zebrafish hearts and applied it to noninjured and regenerating hearts at 7, 14, and 30 days postamputation (dpa). We have then characterized the composition of the zebrafish heart ECM, as well as the major changes in ECM composition that take place during heart regeneration. Finally, we have used atomic force microscopy (AFM) to analyze the effect that changes in ECM composition have on matrix stiffness. Our studies identify important changes in ECM protein composition and mechanical properties during zebrafish heart regeneration.

[1] The abbreviations used are: ECM, extracellular matrix; HA, hyaluronic acid; AFM, atomic force microscopy; VSN, variance stabilization normalization; dpa, days postamputation.

EXPERIMENTAL PROCEEDURES

Animal Maintenance and Surgical Procedure—Wild-type zebrafish of the AB strain were maintained according to Standard protocols (49). The ventricular amputations were done as previously described by Raya *et al.*, 2003 (19). Animal procedures were performed under the approbation of the Ethics Committee on Experimental Animals of the PRBB (CEEA-PRBB).

Ventricle Decellularization—Animals were sacrificed, and hearts were extracted after an intra-abdominal injection of 20 μl of heparin (1000U/ml, Sigma-Aldrich, Madrid, Spain). Only the ventricles were decellularized by immersion in a 0.5% SDS solution for 4h. Then ventricles were washed with distilled H_2O for 30 min. Then immersed into a 1% Triton-X solution for 30 min and finally washed three times with distilled H_2O for 10 min each wash. All solutions were previously filtered with a 0.2 μm filter, and all incubations steps were done in a horizontal shaking plate at 30 °C and 28 rpm.

Tissue Processing and Staining—Zebrafish hearts were extracted as previously mentioned and fixed overnight with 4% paraformaldehyde. Then the hearts were incubated overnight at 4 °C with 30% sucrose and frozen in OCT (Tissue-Tek, Alphen aan den Rijn, The Netherlands) for cryosectioning. The decellularized ventricles were embedded in OCT, snap frozen with isopentane and fixed after sectioning incubating them 10min in 4% paraformaldehyde. 10 μm thick slices of the samples were counterstained with DAPI (1:10,000) for 4 min and stained with Hematoxylin and Eosin, and Masson's Trichrome staining.

Genomic DNA Extraction and Quantification—Genomic DNA was extracted from nondecellularized and decellularized zebrafish ventricles. Samples were homogenized by adding 200 μl of PBS, 20 μl Proteinase K (Qiagen, Madrid, Spain) and 4 μl of RNAseA (Qiagen) and vortexed. Tissue lysis was done adding 200 μl of AL Lysis buffer (Qiagen). DNA was purified by chloroform and precipitated using isopropanol. Finally, the pellets were dried and 20 μl of TE buffer (Qiagen) was added. DNA concentration was measured with a spectrophotometer (NanoDrop® ND-100, Thermo Fisher Scientific, Barcelona, Spain).

Liquid Chromatography-Mass Spectrometric Analysis—Two different proteomic analyses were performed: one to assess the decellularization protocol, and another one to assess the regeneration process. For the first one, native zebrafish ventricles, half-decellularized ventricles, and fully decellularized ventricles were analyzed. For the second one, decellularized zebrafish ventricles at 7 dpa, 14 dpa, and 30 dpa, were analyzed compared with sham operated fishes. Proteins of each sample were solubilized by mixing with 50μl of 1% SDS, 100 mM Tris-HCl pH 7.6, 100 mM DTT, 10 min sonication and boiling for 3 min. Protein extracts were clarified by centrifugation at 16,000 $\times$ *g* for 5 min and quantified using the RcDc kit (BioRad, Hercules, CA). In the first proteomic analysis, 12 μg of protein of each sample were digested with LysC and trypsin using a Filter-Aided Sample Preparation (FASP) protocol and further analyzed by mass spectrometry. The LC separation was conducted on an Easy-nLC 1000 (Thermo) using 0.1% formic acid as Solvent A and acetonitrile with 0.1% formic acid as B. Each run was carried out at 250 nL/min with a gradient of 95% of solvent A to 65% A in 180 min. Blank samples with solvent A injections were run in between each sample. Sample was concentrated in an Acclaim PepMap 100 trap column (Thermo), and fractionated in a Nikkyo Technos Co., 75 μm ID, 3 A pore size, 12.5 cm in length with built in emitter column, coupled to a Nanospray Flex (Thermo) ESI source. Shotgun LC-MS/MS analysis was performed online with an electrospray voltage of 1.9 kV using a Q Exactive HF mass spec-

trometer (Thermo) with HCD fragmentation using top 15 precursor with charge 2 to 5 for data-dependent acquisition (DDA). MS1 spectra were acquired in the mass range 390–1700 *m/z* at a resolution of 60,000 at *m/z* 400 with a target value of 3×10^6 ions and maximum fill time of 20 ms. MS2 spectra were collected with a target ion value of 2×10^5 and maximum 100 ms fill time using a normalized collision energy of 27. Dynamic precursor exclusion was set at 15 s. The raw files were processed with the MaxQuant software (version 1.6.2.6a) using the built-in Andromeda Search Engine. The *Danio rerio* TrEMBL database downloaded from www.uniprot.org (Oct, 8th 2018) (62,078 entries) was used to search for peptides. MS/MS spectra were searched with a first search precursor mass tolerance of 20 ppm. Then, the peptide masses were corrected, and a second search was performed at 4.5 ppm of mass tolerance. The fragment tolerance was set to 0.5 Da, the enzyme was trypsin and a maximum of 2 missed cleavages were allowed. The cysteine carbamidomethylation was set as fixed modification and methionine oxidation as well as protein N-terminal acetylation as variable modifications. To improve the identifications the "match between runs" was enabled among the replicates of every experimental condition.

In the second proteomic analysis, the protein amount recovered was around 5 μg for the 0.5% SDS treated sample. The buffer was changed to 2 M Urea 50 mM Ammonium Bicarbonate using a 5kD Amicon Ultrafiltration device, and the samples were digested with trypsin. Each sample was the analyzed by LC-MS in duplicate. Five hundred nanograms of each sample was analyzed on a Maxis Impact high-resolution Q-TOF spectrometer (Bruker, Bremen, Germany), coupled to a nano-HPLC system (Proxeon, Odense, Denmark). The samples evaporated and dissolved in 5% acetonitrile, 0.1% formic acid in water, were first concentrated on a 100 mm ID, 2 cm Proxeon nanotrapping column and then loaded onto a 75 mm ID, 25 cm Acclaim PepMap nanoseparation column (Dionex, Sunnyvale, CA). Chromatography was run using a 0.1% formic acid - acetonitrile gradient (5–35% in 120min; flow rate 300 nL/min). The column was coupled to the mass spectrometer inlet through a Captive Spray (Bruker) ionization source. MS acquisition was set to cycles of MS (2 Hz), followed by Intensity Dependent MS/MS (2–20 Hz) of the 20 most intense precursor ions with an intensity threshold for fragmentation of 2500 counts, and using a dynamic exclusion time of 0.32min. All spectra were acquired on the range 100–2200Da. LC-MSMS data was analyzed using the Data Analysis 4.0 software (Bruker). Proteins were identified using Mascot (ver. 2.5; Matrix Science, London UK) to search against the *Danio rerio* proteins in the SwissProt 20160108 database (43,095 sequences). MS/MS spectra were searched with a precursor mass tolerance of 10 ppm, fragment tolerance of 0.05 Da, trypsin specificity with a maximum of 2 missed cleavages, cysteine carbamidomethylation set as fixed modification and methionine oxidation as variable modification.

Both mass spectrometry proteomics data sets, for the decellularization protocol and for the regeneration proteome, have been deposited to the ProteomeXchange Consortium (http://proteomecentral.proteomexchange.org) via the PRIDE partner repository (50) with the data set identifiers <PXD011627> and <PXD010092>, respectively.

Criteria for Protein Identification—For the decellularization protocol proteomic analysis, MaxQuant software (version 1.6.2.6a) was used to validate the peptides and proteins identifications. The final list of peptides was obtained after applying a 5% False Discovery Rate (FDR). For proteins, only the proteins with at least 1 assigned peptide after applying a 5% FDR were considered. The nonunique peptides were assigned to the corresponding protein group according to the Razor peptides rule implemented in the software (principle of parsimony). Finally, the identified peptides and proteins were filtered to remove the peptides/proteins tagged as "Reverse" (significantly identified in the reverse database) and "potential contaminant" (items identified as contaminants in the "contaminants.fasta" file) as well as the proteins "Only identified by site" (proteins identified only with modified peptides). The lists can be found in the supplemental material uploaded to the PRIDE repository, with project accession code <PXD011627>.

For the regeneration process proteomic analysis, Scaffold (version Scaffold_4.0.5, Proteome Software Inc., Portland, OR) was used to validate MS/MS based peptide and protein identifications. Peptide identifications were accepted if they could be established at greater than 99% probability by the Peptide Prophet algorithm (51). Protein identifications were accepted if they could be established at greater than 98% probability to achieve an FDR less than 1% and contained at least 1 identified peptide. Protein probabilities were assigned by the Protein Prophet algorithm (52). Protein isoforms and members of a protein family would be identified separately only if peptides that enable differentiation of isoforms had been identified based on generated MS/MS data. Otherwise, Scaffold would group all isoforms under the same gene name. Different proteins that contained similar peptides and which were not distinguishable based on MS/MS data alone were grouped to satisfy the principles of parsimony. The lists of identified peptides and proteins can be found in supplemental Tables S6 and S7, respectively.

Label-free Protein Quantification—For the decellularization protocol proteomic analysis, the proteins were quantified with the help of the label-free algorithm (LFQ) implemented in the MaxQuant software using the unique and razor peptides. The minimum number of peptides to be available in all the pair-wise comparisons was set to 2 and the "stabilize large LFQ ratios" option enabled.

For the proteomic analysis of heart regeneration, relative label-free protein quantification analysis was performed on the different samples analyzed using spectral counting and LFQ (as above). The "Quantitative Value- Total Normalized Spectra" function of Scaffold software was used for quantitative comparison. This function provides the total number of spectra that matched to a protein identified in each sample, after normalizing the values for each sample by a factor calculated so that the total number of normalized spectral counts is identical for all samples, thus correcting for differences in sample load. Only those proteins for which the total sum of spectral counts for the eight runs was greater than 5 were considered for quantitative comparison.

Analysis and Validation of Proteomic Data On Regeneration—In order to annotate proteins associated with Extracellular Matrix we downloaded the GO annotations of zebrafish, human, and mouse organisms from the repository of Gene Ontology Consortium (53, 54). The resulting list of proteins falling into the GO Term GO:0031012 (*i.e.* Extracellular Matrix) was supervised and curated by hand. To determine an enrichment in ECM proteins in or decellularized samples, the proteomics data obtained was compared with the zebrafish proteomic data already published (55) with Panther (pantherdb.org) for ECM protein enrichment. GO enrichment analysis were done with Enrichr tool (version August 24th, 2017). One of the challenges proteomics data generated in a mass spectrometry-based experiment is the presence of missing values. To overcome this drawback, proteins sparsely quantified were removed from the data analysis. In this regard, proteins quantified by more than 5 spectral counts in average across samples, or at least in two thirds of all samples by LFQ, were considered. In the latter case, after normalizing the data, the remaining missing values were imputed by random numbers generated from a normal distribution. To stabilize the variance, variance stabilization normalization (VSN) was applied to both spectral counts and LFQ intensities (56). A hierarchical clustering analysis via 1,000 bootstrap resampling replications was performed, using the R (version 3.2.3) statistical language package pvclust (57), to construct a dendrogram

with correlation distance and average method. Normalized data values were z-scaled by rows in order to build the heatmap. Validation of the proteomic data was performed by qRT-PCR analyzing 3 biological replicates comprised of 5 ventricles each for each time point (7 dpa, 14 dpa, 30 dpa, and sham). RNA was extracted with TriReagent (Molecular Research Center, Inc., Cincinnati, OH) and chloroform, and cDNA was synthesized using the Transcriptor First Strand cDNA Synthesis Kit (Roche, Pleasanton, CA).

Atomic Force Microscopy (AFM) For the Measurement of the Extracellular Matrix—Zebrafish hearts were extracted, included in Optimal Cutting Temperature compound (OCT) and frozen at −80 °C. Then, slices of 25 μm were cut with a cryostat (HM 560, CryoStar Thermo Scientific) and placed on positively charged glass slides and stored at −20 °C. Before measurements, slices were washed with PBS 1× and decellularized to remove all cellular components and preserve the ECM. A detergent-based protocol was used to decellularize the slices. Briefly, slices were immersed in sodium-dodecyl disulfate (SDS) 0.1% during 5 min, followed by 10 min of Triton X-100 1% and finally washed during 20 min with NaCl 0.9% solution. The slices were kept in constant moderate agitation.

Immediately after decellularization process, the samples were measured by AFM. The perimeter of glass slides was outlined with a water repellent marker (Super PAP PEN, Invitrogen, Barcelona, Spain), keeping 1 ml of PBS 1× pooled over the slices. Then, slides were placed on the sample holder of a custom-built AFM coupled to an inverted optical microscope (TE 2000, Nikon, Tokyo, Japan). The Young's modulus (E) of the ECM was measured using V-shaped Au-coated silicon nitride cantilever (nominal spring constant of k = 0.06 N/m) with a spherical polystyrene bead of 2.25 μm radius glued at its end (Novascan Technologies, Ames, IA), which was previously calibrated by thermal tune method. 3-D piezoactuators coupled to strain gauge sensors (Physik Instrumente, Karlsruhe, Germany), allowed to place the cantilever on the region of interest with nanometric resolution and to measure the vertical displacement of the tip (z). The deflection of the cantilever (d) was measured with a quadrant photodiode (S4349, Hamamatsu, Japan) using the optical lever method. The slope of a deflection-displacement curve (d-z) obtained on a bare region of the rigid substrate was used to calibrate the relationship between cantilever deflection and photodiode signal. Therefore, the force exerted by the cantilever was computed as $F = k \cdot d$. The indentation of the sample (δ) was computed as $\delta = (z - z_0) - (d - d_0)$, where z_0 and d_0 are the positions of the contact point. To extract E, F-δ curves were analyzed by the spherical Hertz contact model (58).

Myocardial stiffness was analyzed at 7, 14, and 30 dpa (n = 5 per time point) and in animals with no injury (control, n = 5). For each sample time point two slices were measured. In every slice, measurements were performed in two zones: uninjured and regenerating heart. In each zone, two locations separated by ~500 μm were measured. At each of the two locations, 5 measurements were made separated by ~10 μm. E of each measurement point was the average of five force curves, obtained with ramp amplitude of 5 μm and frequency of 1Hz, resulting in tip velocity of 5 μm/s.

Experimental Design and Statistical Rationale—For LC-MS spectrometric analysis of the decellularization protocol, we used three pools of 3 native zebrafish ventricles per pool, three pools of 10 ventricles after SDS treatment per pool, and three pools of 20 decellularized ventricles per pool. A two-way ANOVA was used for comparing ECM proteins over the decellularization states.

For LC-MS spectrometric analysis during regeneration, 6 ventricles per sample were pooled for 7 dpa, 14 dpa, and 30 dpa. In control samples 8 ventricles were pooled. One-way ANOVA was used to determine the statistical significant differences. Raw p values have been controlled by adjusting the Benjamini-Hochberg false discovery rate (FDR).

Kruskal-Wallis followed by a Dunn's multiple comparisons test was used to determine the qRT-PCR statistical significance of the differences at RNA level between control hearts and hearts at each regeneration time point. Mann-Whitney test was used to determine statistical significance of the differences between uninjured hearts and hearts at each time point on AFM analysis. GraphPad software was used to carry out all the statistics. All results are expressed as mean ± S.E. of mean (S.E.).

RESULTS

Enrichment of Zebrafish Heart ECM Proteins—To study the ECM protein composition of zebrafish ventricles, we developed a decellularization protocol consisting on detergent treatment with 0,5% sodium dodecyl sulfate (SDS), followed by 1% Triton-X 100 to remove SDS prior to processing for analysis (Fig. 1*A*). This treatment produced translucent decellularized scaffolds that structurally resembled the zebrafish ventricle (Fig. 1*B*). Following decellularization, DAPI staining and other histological staining were used to assess the extent of cell removal and the integrity of the ECM. No DAPI staining was seen after treatment (Fig. 1*C*), and spectrophotometric analysis showed an ~80% reduction in DNA content after decellularization of zebrafish hearts (Fig. 1*D*). Moreover, hematoxylin and eosin, and Masson trichrome staining revealed no conspicuous damage to the ECM, while further confirming the absence of nuclei in decellularized samples (Fig. 1*E*). To analyze whether the decellularization process altered the relative abundance of ECM proteins, we characterized the proteome of zebrafish hearts before (native), after SDS treatment, and at the end of decellularization by liquid chromatography-mass spectrometry (LC-MS). A total of 447 unique proteins were detected in native hearts, of which only 15 (3.4%) corresponded to extracellular proteins as annotated by Gene Ontology and manual curation (see Experimental Procedures for details). The numbers of extracellular proteins detected after SDS treatment and at the end of the decellularization protocol increased to 35 and 36, respectively, whereas those of intracellular proteins decreased from 432 in native hearts to 352 after SDS treatment, and 341 in fully decellularized hearts (supplemental Table S1). As expected, decellularization not only decreased the number of intracellular proteins detected, but also their abundance as quantified by peptide peak intensity, whereas the opposite trend was observed for extracellular proteins (Fig. 1*F*). Importantly, all extracellular proteins identified in native hearts were also detected in samples after SDS treatment, and after complete decellularization, demonstrating that the protocol used for decellularizing zebrafish hearts did not introduce bias in our analyses because of preferential removal of specific ECM components. The result of the decellularization protocol was, therefore, an enrichment of ECM proteins at the expense of cytoplasmic and nuclear proteins (Fig. 1*G*). The results of these analyses validate the applicability

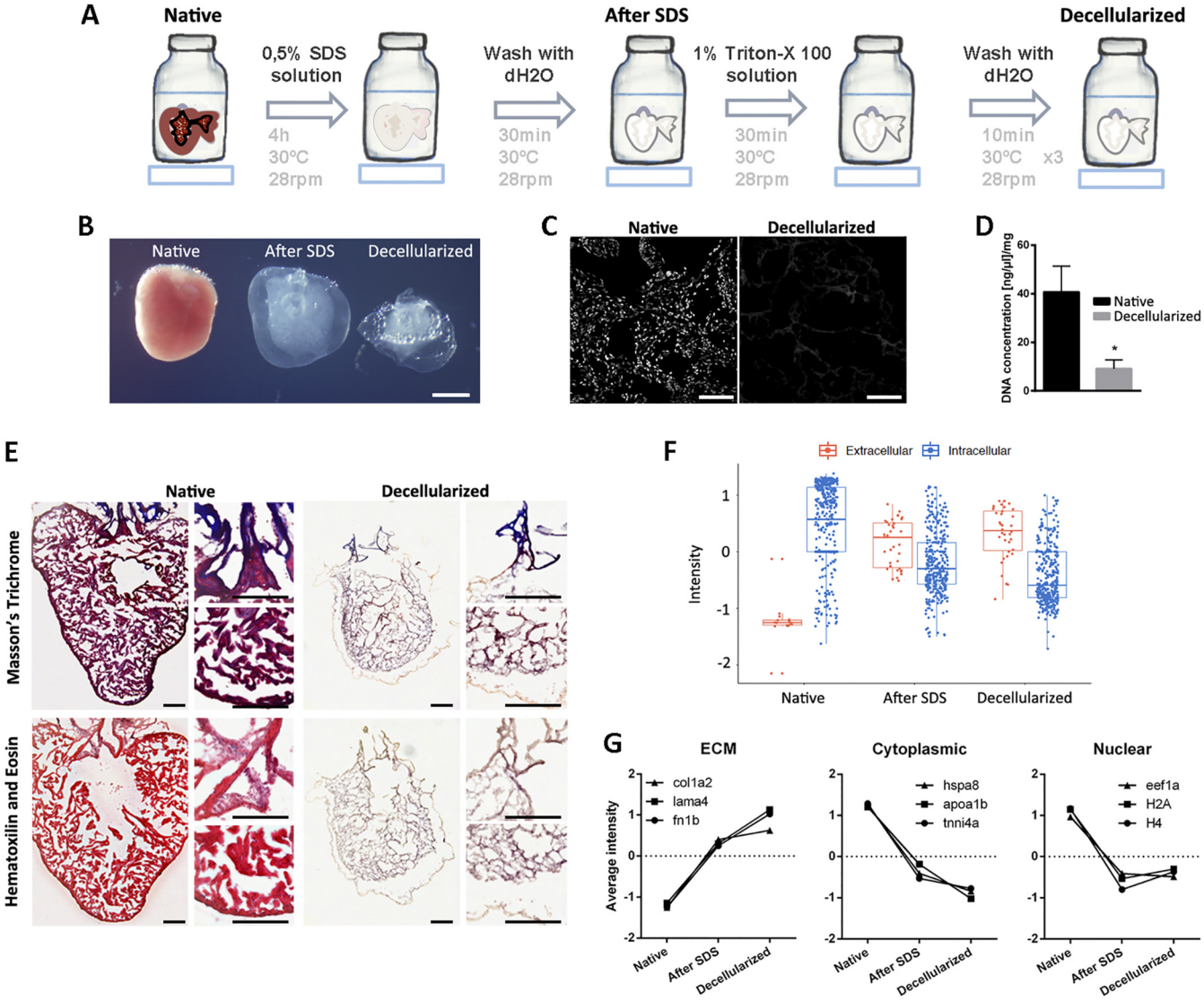

FIG. 1. **Decellularization protocol for zebrafish hearts.** *A*, Representation of the protocol used to decellularize zebrafish ventricles. *B*, Images of the ventricles at different points of the decellularization protocol. From left to right, native ventricle, after 0.5% SDS, and at the end of the decellularization ptotocol (scale bar 500 μm). *C–E*, The efficiency of the decellularization process was characterized by DAPI staining (scale bar 50 μm) (*C*), spectrophotometric quantification of DNA ($n = 3$) (*D*), and Masson's trichrome (*E*, upper images) and Hematoxylin and Eosin (*E*, lower images) staining (scale bar 100 μm). *F*, Box plot representing an overall distribution of the average intensities of each protein in each sample group. ECM proteins and intracellular proteins have been independently plotted to better visualize the effect of decellularization in each class of proteins. *G*, The profile of specific ECM, cytoplasmic and nuclear proteins is plotted, showing loss of intracellular proteins and enrichment of ECM proteins during the decellularization protocol. Statistical significance of DNA content was analyzed with unpaired Student's *t* test. *, $p < 0.05$.

of our zebrafish heart decellularization protocol to enrich for ECM proteins, while not altering the relative abundance of ECM protein components.

Profile of ECM Proteins in Adult Zebrafish Hearts—Proteomics analysis of the decellularized sham zebrafish hearts by LC-MS allowed us to identify a total of 62 proteins with ≥3 spectral counts, of which 25 were ECM proteins (supplemental Table S2). Collagens, fibronectin 1b and fibrinogens were the most abundant proteins in the decellularized zebrafish ventricle proteome. Binding, structural molecule activity, receptor activity, and catalytic activity were the most represented molecular function Gene-Ontology (GO) terms (GO:0005488, GO:0005198, GO:0004872, and GO:0003824, respectively) for these identified ECM proteins. A search for GO enriched terms using Enrichr analysis revealed that the 10 most enriched biological processes in our control proteome (GO:0030199, GO:1905590, GO:0071711, GO:0098784, GO:0010215, GO:0030198, GO:0021820, GO:0061148, GO:0085029, and GO:0022617), were all ECM related (Fig. 2*A*).

We next compared the GO cellular component terms represented in our ECM-enriched zebrafish ventricle proteome with those of whole cardiac zebrafish proteomes previously

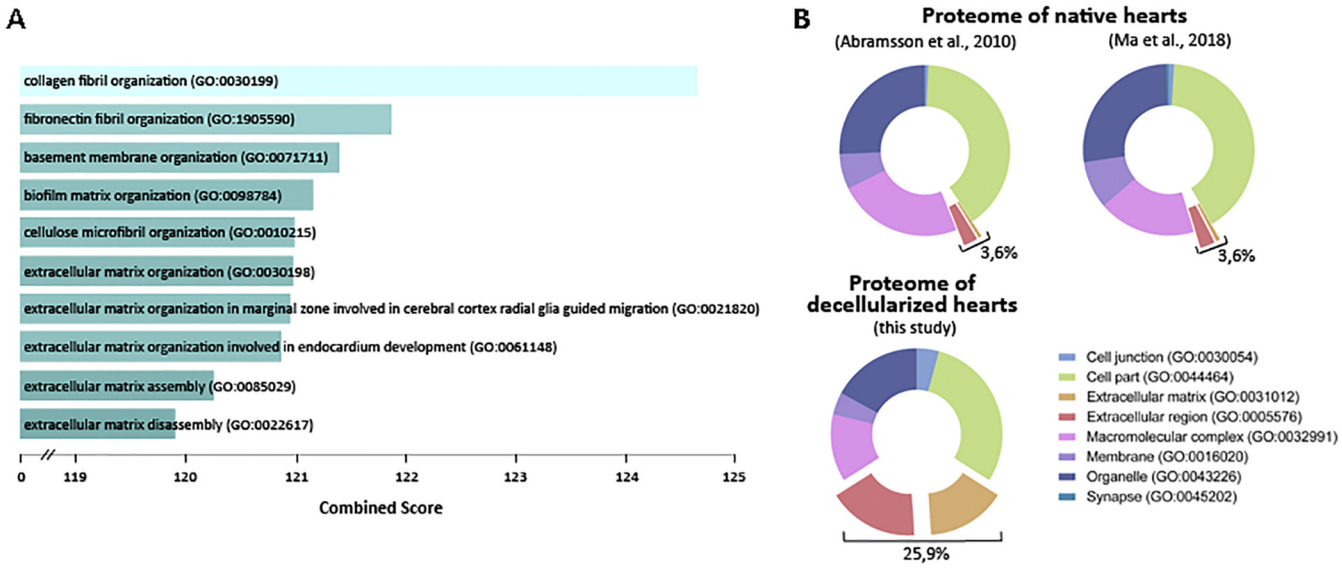

FIG. 2. **Decellularized zebrafish ventricles are enriched in ECM proteins.** *A*, Representation of the 10 most enriched Biological Process GO terms in our proteome of control hearts. Combined score is taken from Enrich program, which takes the log of the *p* value from the Fisher exact test and multiplies it by the z-score of the deviation from the expected rank. *B*, Representation of the Cell Component Gene Ontology (GO) of the published zebrafish heart proteome of Abramsson *et al.* (2010) (55), the published sham heart proteome of Ma *et al.* (2018) (59) and our proteomic analysis of decellularized zebrafish ventricles. Panther assigned GO terms to 138, 1902, and 60 proteins from the proteomes described in Abramsson *et al.* (2010) (55), Ma *et al.* (2018) (59), and the one described here, respectively.

reported by Abramsson *et al.* (55) and Ma *et al.* (59) Analysis by Panther revealed an enrichment of ECM and extracellular region terms in our decellularized samples compared with whole heart proteomes (Fig. 2*B*). These results further confirmed that ventricle decellularization allows a better detection of changes in ECM protein composition.

Changes in ECM Protein Composition During Zebrafish Heart Regeneration—To determine whether ECM protein composition changes during zebrafish heart regeneration, we also analyzed with LC-MS decellularized ventricle samples of zebrafish hearts at 7, 14, and 30 dpa. Considering the limitations of spectral counting for proteins associated with low values, we also used label-free quantitation (LFQ)-based on peak intensities for this purpose. We detected a total of 245 proteins among all samples by spectral counting, and 387 proteins by LFQ analysis (supplemental Table S2). Of these, 120 proteins were represented by >5 spectral counts across sample averages, or had LFQ intensity values detected in over 2/3 of the samples (supplemental Tables S3 and S4). From these 120 proteins, 32 corresponded to extracellular proteins and 88 to intracellular proteins. Of note, 23 out of the 50 most abundant proteins found in these analyses were ECM proteins (supplemental Tables S3 and S4). Heatmap representation of protein profiles showed large differences between control and 7-dpa samples. However, profile changes among other regeneration time points were less evident (Fig. 3*A*). Overall, hierarchical clustering analysis grouped sample replicates together for all time points with good Approximately Unbiased *p* values (AU) indexes. Regenerating hearts clustered together, with 30-dpa samples being closer to control and away from 7-and 14-dpa samples (Fig. 3*B*). ANOVA analysis revealed that 36 out of the overall 120 proteins detected showed statistically significant changes during regeneration, of which 18 were ECM proteins (supplemental Table S5). Among the ECM proteins whose levels changed significantly during regeneration, fibrinogen a, b, and g, as well as fibronectin 1b and periostin b, showed a peak at 7 dpa. In contrast, the levels of collagens and fibrillin 2b showed a statistically significant decrease during regeneration, which was more evident at 7 dpa.

To ascertain if changes in protein abundance were the result of differential gene expression, we measured by quantitative reverse transcription polymerase chain reaction (qRT-PCR) the expression level of 6 genes encoding ECM proteins that change in abundance during regeneration. We found positive correlation between mRNA and protein levels in the case of fibronectin/*fn1b* and periostin b/*postnb*, in which increased transcription levels were also found peaking at 7 dpa (Fig. 3*C*–3*D*). However, expression levels of *col4a2*, *col5a1*, *col5a2a*, and *fbn2b* were all found to be up-regulated at 7dpa (Fig. 3*E*–3*H*), in contrast with the decreased protein levels found in regenerating heart ECM (supplemental Table S5). This suggests that changes in fn1b and postnb protein levels during regeneration are regulated transcriptionally, whereas the regulation of *col4a2*, *col5a1*, *col5a2a*, and *fbn2b* would be posttranscriptional.

Changes in ECM Biomechanical Properties During Zebrafish Heart Regeneration—Changes in ECM protein composition can result in modifications in the biomechanical properties of the matrix. AFM allowed us to measure and

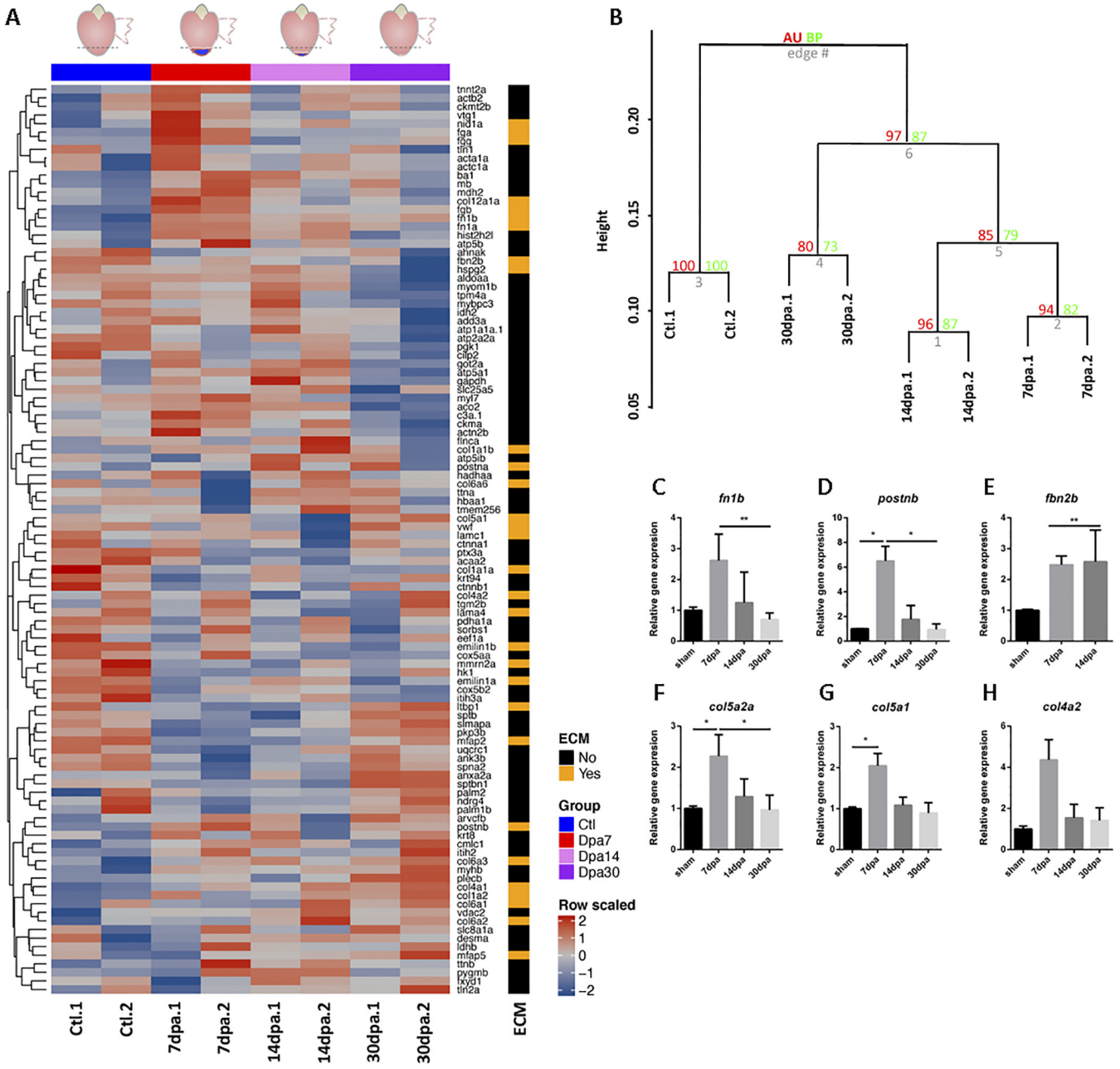

FIG. 3. **Changes in ECM protein composition during heart regeneration.** *A*, Heat-map for the 96 proteins detected across samples in zebrafish control decellularized hearts (Ctl) and at different time points of regeneration. The time points analyzed were 7 dpa, 14 dpa, and 30 dpa. Red indicates increased protein expression and blue indicates reduced protein expression. The ECM column indicates the ECM proteins in orange. Data are row scaled. *B*, Hierarchical clustering with bootstrap analysis of all the samples. AU, Approximately Unbiased *p* value; BP, Bootstrap Probability value. *C–H*, Gene expression assessment by real time qPCR of the ECM proteins significantly changing in the proteomic analysis during the regeneration process. *fn1b*, fibronectin 1b; *postnb*, periostin b; *col5a1*, collagen type 5 α1 chain; *col4a2*, collagen type 4 α2 chain; *col5a2a*, collagen type 5 α2a chain; *fbn2b*, fibrillin 2b. Significance was analyzed with Kruskal-Wallis followed by a Dunn's multiple comparisons test. *, $p < 0.05$; **, $p < 0.01$.

compare the stiffness of the ECM during heart regeneration (Fig. 4). For this purpose, 25-μm thick slices of control or regenerating zebrafish hearts were decellularized and the ECM regions of interest identified by phase contrast microscopy (Fig. 4*A*–4*C*). The Young's modulus of control zebrafish ventricle ECM was calculated at 8.1 $\pm$ 1.7 kPa. We then compared these values with those of regenerating hearts at 7 and 14 dpa (Fig. 4*D*). We chose these time points because our proteomic analysis had revealed the major ECM changes at 7 dpa (Fig. 3*A* and 3*B*, and supplemental Tables S3 and S4). AFM measures of the noninjured myocardium and the regenerating area revealed an overall sig-

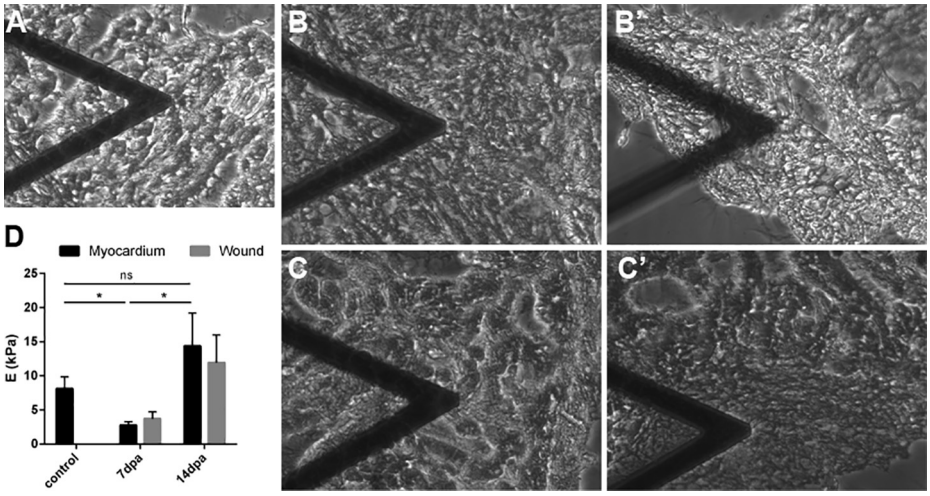

FIG. 4. **Stiffness of the extracellular matrix of regenerating hearts.** *A–C*, Bright field images of decellularized zebrafish hearts being analyzed by AFM at the myocardium away from the injury area. *B'–C'*, Bright field images of decellularized zebrafish hearts being analyzed by AFM at the regenerating area. *A*, Control decellularized heart, *B*, *B'*, 7 dpa decellularized hearts, *C*, *C'*, 14 dpa decellularized heart. The triangular shape in *A–C* and *B'–C'* is the AFM cantilever. E, Young's modulus of the heart ECM of noninjured, 7 dpa, and 14 dpa hearts ($n = 5$ each). dpa, Days postamputation. Statistically significance was assessed with Man-Whitney test. *, $p < 0.05$.

nificant decrease of the ventricular ECM stiffness at 7 dpa (myocardium 2.8 ± 0.5 kPa and wound 3.7 ± 1.0 kPa). The stiffness of decellularized ventricles returned to control values by 14 dpa (myocardium 14.4 ± 4.8 kPa and wound 11.9 ± 4.0 kPa). No significant differences were detected between the noninjured myocardium and the regenerating area in any time points analyzed, suggesting that the ECM changes observed take place at the organ level.

DISCUSSION

ECM remodeling is a critical step in development, wound healing and regeneration (31, 38, 40, 41, 60). The present study characterized the ECM composition and its changes during zebrafish regeneration. We have developed a decellularization protocol for zebrafish ventricles that results in ECM enrichment, as well as facilitating the analysis of the proteomic profile of the zebrafish ventricle ECM. Moreover, we have analyzed the ECM changes during heart regeneration and assessed the stiffness of the ECM at different time points of this process. Altogether, the results from our studies should help better understanding the role of the ECM in zebrafish heart regeneration.

The ECM composition has not been fully studied and described in the specific contexts of the zebrafish heart and cardiac regeneration. Few are the studies done to analyze the ECM in the zebrafish heart. The proteome of different zebrafish organs, including the heart, were analyzed by Abramsson and colleagues and only 4 collagen proteins were detected in the heart proteome (55). In the present study, we have described the presence of 7 additional collagens (col1a2, col1a1b, col6a2, col4a1, col4a2, col5a2a, and col6a6) in control samples, corroborating that they are the main structural element of the zebrafish heart ECM. Collagens provide tensile strength, regulate cell adhesion, support chemotaxis and migration, and direct tissue development (61). Recently Chen and colleagues analyzed the decellularized ECM of zebrafish heart using a mechanical decellularizing approach (62). They qualitatively described the presence of 4 ECM proteins, of which we detect 3 as well as 21 new ones. Thus, our decellularization process followed by LC/MS analysis provided a more comprehensive, as well as quantitative, method to define the ventricular ECM of the zebrafish.

In terms of the cardiac regeneration process, there was no study to our knowledge that analyzed the importance of the ECM itself in the zebrafish cardiac regeneration model. Transcriptomic and proteomic approaches have sought to profile the whole gene expression and protein changes during zebrafish heart regeneration. The former identified gene expression changes during regeneration process and described an increase of transcripts related with secreted molecules, catepsins and metalloproteinases, and wound response/inflammatory factors (45, 46). Also, transcripts coding for ECM and adhesion molecules were detected to be commonly and differentially expressed when comparing the transcriptomes of zebrafish regenerating hearts and fins (46). On the other hand, proteomic studies have been mainly performed on native cardiac samples without decellularization before protein detection, where ECM proteins could be masked by the large amount of intracellular proteins (31, 32, 59, 62). Moreover, these previous proteomic studies have focused on early regenerating time points and do not provide an overview of the proteomic changes during the entire regenerating process (32, 62).

It is also worth noting that, in our studies, ECM proteins were overrepresented among those that showed significant changes in abundance during heart regeneration. Thus, enrichment analysis using Enrichr tool on all proteins that showed significant changes during regeneration identified Biological Process GO terms related with ECM as the most represented (supplemental Fig. 1*A*). In contrast, a similar analysis of published proteomic data (59) only identified enrichment of the ECM-related GO terms fibrinolysis (GO:0042730) and plasminogen activation (GO:0031639), and not among the most enriched in that data set. A summary of the 10

most-enriched Biological Process GO terms during zebrafish heart regeneration identified in our studies and in those of Ma and colleagues (59) is presented in supplemental Fig. 1*B*.

Both transcriptomic and proteomic studies have identified some ECM proteins important during regeneration. Wang and colleagues described the importance of fibronectin during regeneration after ventricular resection, suggesting a positive effect on cardiomyocyte migration (31). Also, tenascin C has been found to be expressed at the border zone and suggested to mediate loosening of cardiomyocyte attachment to the substrate, thereby facilitating cardiomyocyte migration (21). Another proteomic study identified the hyaluronic acid receptor (Hmmr) to be important for the epicardium EMT migration toward the injury (32). All these suggest that tissue remodeling and ECM dynamics are important factors during zebrafish heart regeneration.

The fact that our analyses did not detect changes in some ECM proteins found in previous studies, such as tnc, may be because of technical limitations. In LC-MS-based analyses, signals of abundant proteins such as collagens and structural proteins can mask the signals of low-abundance proteins. Also, new proteomic analytical tools have been developed, but we strongly believe that proteomic analysis of ECM enriched samples is a powerful approach to study the ECM components in heart regeneration. In this study we have identified the main changes in ECM protein composition during zebrafish heart regeneration. Decreased amounts of collagen IV, collagen V, collagen VI, and fibrillin 2b, as well as increased amounts of fibrinogens, fibronectin 1b and periostin b comprise the initial regenerating ECM. We have been also able to detect proteins that were not previously detected in any transcriptomic or proteomic study, such as col4a2 and fbn2b. Two groups of proteins appear to be regulated differently. In the first group, positive correlation between protein abundance and gene expression in the case of fn1b and postnB, indicates a transcriptional regulation of these genes during heart regeneration (37, 46). In the second group, decreased levels of col4a2, col5a1, col5a2a and fbn2b proteins inversely correlate with gene expression, which we interpret as a regulatory feedback mechanism to recover the protein levels.

Stiffness is itself a mechanical property of the ECM. It is known to be involved in cell processes such as the regulation of cell proliferacion (43, 63), dedifferentiation (43), migration (through durotaxis) (64) and stem cell differentiation (65). We analyzed the stiffness of the regenerating zebrafish ventricle and found a significant decrease in ECM stiffness at 7 dpa. It is known that an increase in collagen concentration or cross-linking is associated with stiffer myocardium (66), whereas an extensive degradation of myocardial collagen is associated with a decrease in ventricular stiffness (66, 67). Thus, this result correlates well with the decrease in abundance of several collagens identified in our proteomic analyses, although further research will be necessary to ascertain if these two findings are, indeed, causally related. An unexpected finding of our mechanical characterization of the regenerating heart ECM was that we did not detect any conspicuous differences in stiffness between the regenerating area and the noninjured myocardium located far away from the lesion. This suggests that changes in ECM composition result in organ-wide effects at the biomechanical level. Interestingly, recent data from our laboratories have identified a low ECM stiffness as a permissive factor regulating the heart regeneration ability of neonatal mice (68). The exact mechanism(s) by which ECM stiffness regulates heart regeneration competence in adult zebrafish and/or neonatal mice require further investigation.

Changes in ECM composition and stiffness are likely to instruct specific cell behaviors and may also trigger further changes in the properties of the ECM itself. The ability of the zebrafish cardiac ECM to induce mammal heart regeneration has been very recently assessed by Chen and colleagues (62). They observed that the zebrafish cardiac ECM exhibited pro-proliferative and chemotactic effects *in vitro* and contributed to a higher cardiac contractile function in mouse. In general, fibrillins are known to play important roles in TGFβ signaling by controlling the amounts of cytokines and in endocardium morphogenesis (69, 70). Signaling by the TGFβ/Activin pathway is known to promote cardiomyocyte proliferation and deposition of ECM proteins (71). Moreover, fibronectin 1b promotes cardiomyocyte migration during zebrafish cardiac regeneration (31). Periostin stimulates healing after myocardial infarction in mice through induction of cardiomyocyte proliferation, and it is known to be responsible of collagen cross-linking (covalent linkage of collagen fibers) (72, 73). Collagen cross-linking, in turn, increases at the same time the accumulation of collagen, matrix rigidity and resistance to degradation (74, 75). Further studies to clarify in detail the function of each ECM protein during cardiac regeneration may lead to a better understanding of this process, and to the development of new avenues for therapeutic intervention to promote regeneration of the mammalian heart.

Acknowledgments—We would like to thank Adriana Rodriguez-Marí and Isil Tekeli for their kind help in the initial phases of this project; and IDIBELL Clinical Proteomics Unit, Bellvitge Biomedical Research Institute (IDIBELL) for the decellularization protocol proteomic analysis.

DATA AVAILABILITY

The raw mass spectrometry proteomics data sets for the decellularization protocol and the regeneration proteome have been deposited to the ProteomeXchange Consortium (http://proteomecentral.proteomexchange.org) via the PRIDE partner repository (50) with the data set identifiers PXD011627 and PXD010092, respectively.

* A.G.-P. was partially supported by a pre-doctoral fellowship from FPI program of the Spanish Ministry of Economy and Competitiveness (MINECO). Additional support was provided by grants from MINECO (RTI2018-095377-B-I00), Instituto de Salud Carlos III-ISCIII/

FEDER (Red de Terapia Celular - TerCel RD16/0011/0024), Generalitat de Catalunya-AGAUR (2017-SGR-899), Fundació La Marató de TV3 (201534-30), PERIS (SLT002/16/00234), and CERCA Programme/Generalitat de Catalunya. The Proteomics Laboratory at VHIO and the IDIBELL Clinical Proteomics Unit belong to ProteoRed, PRB2-ISCIII, supported by grant PT13/0001.

S This article contains supplemental Tables. We declare we have no competing interests.

|||| To whom correspondence should be addressed. Tel.: +34 933 160 320; Fax: +34 933 160 332; E-mail: araya@cmrb.eu.

Author contributions: A.G.-P., D.N., F.C., and A.R. designed research; A.G.-P., S.J.-D., C.G.-P., I.J., D.N., and F.C. performed research; A.G.-P., J.L.M., S.J.-D., D.N., F.C., and A.R. analyzed data; A.G.-P. and A.R. wrote the paper.

REFERENCES

1. Mendis, S., Puska, P., and Norrving, B. (2011) Global Atlas on cardiovascular disease prevention and control. *World Heal. Organ. Geneva*, **164**
2. Kathiresan, S., and Srivastava, D. (2012) Genetics of human cardiovascular disease. *Cell* **148,** 1242–1257
3. Beltrami, A. P., Urbanek, K., Kajstura, J., Yan, S.-M., Finato, N., Bussani, R., Nadal-Ginard, B., Silvestri, F., Leri, A., Beltrami, C. A., and Anversa, P. (2001) Evidence That Human Cardiac Myocytes Divide after Myocardial Infarction. *N. Engl. J. Med.* **344,** 1750–1757
4. Kajstura, J., Leri, A., Finato, N., Di Loreto, C., Beltrami, C. A., and Anversa, P. (1998) Myocyte proliferation in end-stage cardiac failure in humans. *Proc. Natl. Acad. Sci. U.S.A.* **95,** 8801–8805
5. Senyo, S. E., Steinhauser, M. L., Pizzimenti, C. L., Yang, V. K., Cai, L., Wang, M., Wu, T.-D., Guerquin-Kern, J.-L., Lechene, C. P., and Lee, R. T. (2013) Mammalian heart renewal by pre-existing cardiomyocytes. *Nature* **493,** 433–436
6. Ma, Y., de Castro Brás, L. E., Toba, H., Iyer, R. P., Hall, M. E., Winniford, M. D., Lange, R. A., Tyagi, S. C., and Lindsey, M. L. (2014) Myofibroblasts and the extracellular matrix network in post-myocardial infarction cardiac remodeling. *Pflugers Arch.* **466,** 1113–1127
7. Holmes, J. W., Borg, T. K., and Covell, J. W. (2005) Structure and mechanics of healing myocardial infarcts. *Annu. Rev. Biomed. Eng.* **7,** 223–253
8. Drenckhahn, J.-D., Schwarz, Q. P., Gray, S., Laskowski, A., Kiriazis, H., Ming, Z., Harvey, R. P., Du, X.-J., Thorburn, D. R., and Cox, T. C. (2008) Compensatory growth of healthy cardiac cells in the presence of diseased cells restores tissue homeostasis during heart development. *Dev. Cell* **15,** 521–533
9. Porrello, E. R., Mahmoud, A. I., Simpson, E., Hill, J. A., Richardson, J. A., Olson, E. N., and Sadek, H. A. (2011) Transient regenerative potential of the neonatal mouse heart. *Science* **331,** 1078–1080
10. Bryant, D. M., O'Meara, C. C., Ho, N. N., Gannon, J., Cai, L., and Lee, R. T. (2015) A systematic analysis of neonatal mouse heart regeneration after apical resection. *J. Mol. Cell. Cardiol.* **79,** 315–318
11. Sen, S., and Sadek, H. A. (2015) Neonatal heart regeneration: Mounting support and need for technical standards. *J. Am. Heart Assoc.* **4,** 3–5
12. Andersen, D. C. C., Ganesalingam, S., Jensen, C. H. H., and Sheikh, S. P. P. (2014) Do neonatal mouse hearts regenerate following heart apex resection? *Stem Cell Reports* **2,** 406–413
13. Andersen, D. C., Jensen, C. H., Baun, C., Hvidsten, S., Zebrowski, D. C., Engel, F. B., and Sheikh, S. P. (2016) Persistent scarring and dilated cardiomyopathy suggest incomplete regeneration of the apex resected neonatal mouse myocardium–A 180 days follow up study. *J. Mol. Cell. Cardiol.* **90,** 47–52
14. Neff, A. W., Dent, A. E., and Armstrong, J. B. (1996) Heart development and regeneration in urodeles. *Int. J. Dev. Biol.* **40,** 719–725
15. Brockes, J. P., and Gates, P. B. (2014) Mechanisms underlying vertebrate limb regeneration: lessons from the salamander. *Biochem. Soc. Trans.* **42,** 625–630
16. Oberpriller, J. O., and Oberpriller, J. C. (1974) Response of the adult newt ventricle to injury. *J. Exp. Zool.* **187,** 249–253
17. Godwin, J. W., and Rosenthal, N. (2014) Scar-free wound healing and regeneration in amphibians: immunological influences on regenerative success. *Differentiation.* **87,** 66–75
18. Jopling, C., Sleep, E., Raya, M., Martí, M., Raya, A., and Izpisúa Belmonte, J. C. (2010) Zebrafish heart regeneration occurs by cardiomyocyte dedifferentiation and proliferation. *Nature* **464,** 606–609
19. Raya, A., Koth, C. M., Büscher, D., Kawakami, Y., Itoh, T., Raya, R. M., Sternik, G., Tsai, H.-J., Rodríguez-Esteban, C., and Izpisúa-Belmonte, J. C. (2003) Activation of Notch signaling pathway precedes heart regeneration in zebrafish. *Proc. Natl. Acad. Sci. U.S.A.* **100,** 11889–11895
20. González-Rosa, J. M., and Mercader, N. (2012) Cryoinjury as a myocardial infarction model for the study of cardiac regeneration in the zebrafish. *Nat. Protoc.* **7,** 782–788
21. Chablais, F., Veit, J., Rainer, G., and Jaźwińska, A. (2011) The zebrafish heart regenerates after cryoinjury-induced myocardial infarction. *BMC Dev. Biol.* **11,** 21
22. González-Rosa, J. M., Martín, V., Peralta, M., Torres, M., and Mercader, N. (2011) Extensive scar formation and regression during heart regeneration after cryoinjury in zebrafish. *Development* **138,** 1663–1674
23. Schnabel, K., Wu, C.-C., Kurth, T., and Weidinger, G. (2011) Regeneration of Cryoinjury Induced Necrotic Heart Lesions in Zebrafish Is Associated with Epicardial Activation and Cardiomyocyte Proliferation. *PLoS ONE* **6,** e18503
24. Wang, J., Panáková, D., Kikuchi, K., Holdway, J. E., Gemberling, M., Burris, J. S., Singh, S. P., Dickson, A. L., Lin, Y.-F., Sabeh, M. K., Werdich, A. A., Yelon, D., Macrae, C. A., and Poss, K. D. (2011) The regenerative capacity of zebrafish reverses cardiac failure caused by genetic cardiomyocyte depletion. *Development* **138,** 3421–3430
25. Xiao, C., Gao, L., Hou, Y., Xu, C., Chang, N., Wang, F., Hu, K., He, A., Luo, Y., Wang, J., Peng, J., Tang, F., Zhu, X., and Xiong, J.-W. (2016) Chromatin-remodelling factor Brg1 regulates myocardial proliferation and regeneration in zebrafish. *Nat. Commun.* **7,** 13787
26. Itou, J., Oishi, I., Kawakami, H., Glass, T. J., Richter, J., Johnson, A., Lund, T. C., and Kawakami, Y. (2012) Migration of cardiomyocytes is essential for heart regeneration in zebrafish. *Development* **139,** 4133–4142
27. Tekeli, I., Garcia-Puig, A., Notari, M., García-Pastor, C., Aujard, I., Jullien, L., and Raya, A. (2017) Fate predetermination of cardiac myocytes during zebrafish heart regeneration. *Open Biol.* **7,** 170116
28. Lepilina, A., Coon, A. N., Kikuchi, K., Holdway, J. E., Roberts, R. W., Burns, C. G., and Poss, K. D. (2006) A dynamic epicardial injury response supports progenitor cell activity during zebrafish heart regeneration. *Cell* **127,** 607–619
29. González-Rosa, J. M., Peralta, M., and Mercader, N. (2012) Pan-epicardial lineage tracing reveals that epicardium derived cells give rise to myofibroblasts and perivascular cells during zebrafish heart regeneration. *Dev. Biol.* **370,** 173–186
30. Cao, J., and Poss, K. D. (2016) Explant culture of adult zebrafish hearts for epicardial regeneration studies. *Nat. Protoc.* **11,** 872–881
31. Wang, J., Karra, R., Dickson, A. L., and Poss, K. D. (2013) Fibronectin is deposited by injury-activated epicardial cells and is necessary for zebrafish heart regeneration. *Dev. Biol.* **382,** 427–435
32. Missinato, M. A., Tobita, K., Romano, N., Carroll, J. A., and Tsang, M. (2015) Extracellular component hyaluronic acid and its receptor Hmmr are required for epicardial EMT during heart regeneration. *Cardiovasc. Res.* **107,** 487–498
33. Sánchez-Iranzo, H., Galardi-Castilla, M., Sanz-Morejón, A., González-Rosa, J. M., Costa, R., Ernst, A., Sainz de Aja, J., Langa, X., and Mercader, N. (2018) Transient fibrosis resolves via fibroblast inactivation in the regenerating zebrafish heart. *Proc. Natl. Acad. Sci. U.S.A.* **115,** 4188–4193
34. Hynes, R. O. (2014) Stretching the boundaries of extracellular matrix research. *Nat. Rev. Mol. Cell Biol.* **15,** 761–763
35. Kim, S.-H., Turnbull, J., and Guimond, S. (2011) Extracellular matrix and cell signalling: the dynamic cooperation of integrin, proteoglycan and growth factor receptor. *J. Endocrinol.* **209,** 139–151
36. Lu, P., Takai, K., Weaver, V. M., and Werb, Z. (2011) Extracellular matrix degradation and remodeling in development and disease. *Cold Spring Harb. Perspect. Biol.* **3,** a005058
37. Le Trinh, A., and Stainier, D. Y. (2004) Fibronectin regulates epithelial organization during myocardial migration in zebrafish. *Dev. Cell* **6,** 371–382
38. Bonnans, C., Chou, J., and Werb, Z. (2014) Remodelling the extracellular matrix in development and disease. *Nat. Rev. Mol. Cell Biol.* **15,** 786–801
39. Lu, P., Weaver, V. M., and Werb, Z. (2012) The extracellular matrix: a dynamic niche in cancer progression. *J. Cell Biol.* **196,** 395–406

40. Dobaczewski, M., Gonzalez-Quesada, C., and Frangogiannis, N. G. (2010) The extracellular matrix as a modulator of the inflammatory and reparative response following myocardial infarction. *J. Mol. Cell. Cardiol.* **48,** 504–511
41. Jessen, J. R. (2015) Recent advances in the study of zebrafish extracellular matrix proteins. *Dev. Biol.* **401,** 110–121
42. Guilak, F., Cohen, D. M., Estes, B. T., Gimble, J. M., Liedtke, W., and Chen, C. S. (2009) Control of stem cell fate by physical interactions with the extracellular matrix. *Cell Stem Cell* **5,** 17–26
43. Yahalom-Ronen, Y., Rajchman, D., Sarig, R., Geiger, B., and Tzahor, E. (2015) Reduced matrix rigidity promotes neonatal cardiomyocyte dedifferentiation, proliferation and clonal expansion. *Elife* **4,** e07455
44. Mercer, S. E., Odelberg, S. J., and Simon, H.-G. (2013) A dynamic spatiotemporal extracellular matrix facilitates epicardial-mediated vertebrate heart regeneration. *Dev. Biol.* **382,** 457–469
45. Lien, C.-L., Schebesta, M., Makino, S., Weber, G. J., and Keating, M. T. (2006) Gene expression analysis of zebrafish heart regeneration. *PLos Biol.* **4,** e260
46. Sleep, E., Boué, S., Jopling, C., Raya, M., Raya, A., and Izpisua Belmonte, J. C. (2010) Transcriptomics approach to investigate zebrafish heart regeneration. *J. Cardiovasc. Med.* **11,** 369–380
47. Sallin, P., de Preux Charles, A.-S., Duruz, V., Pfefferli, C., and Jaźwińska, A. (2015) A dual epimorphic and compensatory mode of heart regeneration in zebrafish. *Dev. Biol.* **399,** 27–40
48. Jaźwińska, A., and Sallin, P. (2016) Regeneration versus scarring in vertebrate appendages and heart. *J. Pathol.* **238,** 233–246
49. Westerfield, M. (2000) *The Zebrafish Book. A Guide for the Laboratory Use of Zebrafish (Danio rerio*) ed University of Oregon Press E (Eugene). 4th Ed.
50. Vizcaíno, J. A., Côté, R. G., Csordas, A., Dianes, J. A., Fabregat, A., Foster, J. M., Griss, J., Alpi, E., Birim, M., Contell, J., O'Kelly, G., Schoenegger, A., Ovelleiro, D., Pérez-Riverol, Y., Reisinger, F., Ríos, D., Wang, R., and Hermjakob, H. (2012) The Proteomics Identifications (PRIDE) database and associated tools: status in 2013. *Nucleic Acids Res.* **41,** D1063–D1069
51. Keller, A., Nesvizhskii, A. I., Kolker, E., and Aebersold, R. (2002) Empirical statistical model to estimate the accuracy of peptide identifications made by MS/MS and database search. *Anal. Chem.* **74,** 5383–5392
52. Nesvizhskii, A. I., Keller, A., Kolker, E., and Aebersold, R. (2003) A statistical model for identifying proteins by tandem mass spectrometry. *Anal. Chem.* **75,** 4646–4658
53. Ashburner, M., Ball, C. A., Blake, J. A., Botstein, D., Butler, H., Cherry, J. M., Davis, A. P., Dolinski, K., Dwight, S. S., Eppig, J. T., Harris, M. A., Hill, D. P., Issel-Tarver, L., Kasarskis, A., Lewis, S., Matese, J. C., Richardson, J. E., Ringwald, M., Rubin, G. M., and Sherlock, G. (2000) Gene ontology: tool for the unification of biology. The Gene Ontology Consortium. *Nat. Genet.* **25,** 25–29
54. The Gene Ontology Consortium. (2017) Expansion of the Gene Ontology knowledgebase and resources. *Nucleic Acids Res.* **45,** D331–D338
55. Abramsson, A., Westman-Brinkmalm, A., Pannee, J., Gustavsson, M., von Otter, M., Blennow, K., Brinkmalm, G., Kettunen, P., and Zetterberg, H. (2010) Proteomics profiling of single organs from individual adult zebrafish. *Zebrafish* **7,** 161–168
56. Huber, W., von Heydebreck, A., Sültmann, H., Poustka, A., and Vingron, M. (2002) Variance stabilization applied to microarray data calibration and to the quantification of differential expression. *Bioinformatics* **18** (Suppl. 1), S96–S104
57. Suzuki, R., and Shimodaira, H. (2006) Pvclust: an R package for assessing the uncertainty in hierarchical clustering. *Bioinformatics* **22,** 1540–1542
58. Jorba, I., Uriarte, J. J., Campillo, N., Farré, R., and Navajas, D. (2017) Probing micromechanical properties of the extracellular matrix of soft tissues by atomic force microscopy. *J. Cell. Physiol.* **232,** 19–26
59. Ma, D., Tu, C., Sheng, Q., Yang, Y., Kan, Z., Guo, Y., Shyr, Y., Scott, I. C., and Lou, X. (2018) Dynamics of zebrafish heart regeneration using an HPLC-ESI-MS/MS approach. *J. Proteome Res*. **17,** 1300–1308
60. Bayomy, A. F., Bauer, M., Qiu, Y., and Liao, R. (2012) Regeneration in heart disease - Is ECM the key? *Life Sci.* **91,** 823–827
61. Frantz, C., Stewart, K. M., and Weaver, V. M. (2010) The extracellular matrix at a glance. *J. Cell Sci.* **123,** 4195–4200
62. Chen, W. C. W., Wang, Z., Missinato, M. A., Park, D. W., Long, D. W., Liu, H.-J., Zeng, X., Yates, N. A., Kim, K., and Wang, Y. (2016) Decellularized zebrafish cardiac extracellular matrix induces mammalian heart regeneration. *Sci. Adv.* **2,** e1600844
63. Balestrini, J. L., Chaudhry, S., Sarrazy, V., Koehler, A., and Hinz, B. (2012) The mechanical memory of lung myofibroblasts. *Integr. Biol.* **4,** 410–421
64. Lo, C.-M., Wang, H.-B., Dembo, M., and Wang, Y. (2000) Cell movement is guided by the rigidity of the substrate. *Biophys. J.* **79,** 144–152
65. Wen, J. H., Vincent, L. G., Fuhrmann, A., Choi, Y. S., Hribar, K. C., Taylor-Weiner, H., Chen, S., and Engler, A. J. (2014) Interplay of matrix stiffness and protein tethering in stem cell differentiation. *Nat. Mater.* **13,** 979–987
66. Brower, G. L., Gardner, J. D., Forman, M. F., Murray, D. B., Voloshenyuk, T., Levick, S. P., and Janicki, J. S. (2006) The relationship between myocardial extracellular matrix remodeling and ventricular function. *Eur. J. Cardio-thoracic Surg.* **30,** 604–610
67. Mujumdar, V. S., Smiley, L. M., and Tyagi, S. C. (2001) Activation of matrix metalloproteinase dilates and decreases cardiac tensile strength. *Int. J. Cardiol.* **79,** 277–286
68. Notari, M., Ventura-Rubio, A., Bedford-Guaus, S. J., Jorba, I., Mulero, L., Navajas, D., Martí, M., and Raya Á. (2018) The local microenvironment limits the regenerative potential of the mouse neonatal heart. *Sci. Adv*. **4,** eaao5553
69. Dietz, H. C. (2010) TGF-β in the pathogenesis and prevention of disease: a matter of aneurysmic proportions. *J. Clin. Invest.* **120,** 403–406
70. Mellman, K., Huisken, J., Dinsmore, C., Hoppe, C., and Stainier, D. Y. (2012) Fibrillin-2b regulates endocardial morphogenesis in zebrafish. *Dev. Biol.* **372,** 111–119
71. Chablais, F., and Jazwinska, A. (2012) The regenerative capacity of the zebrafish heart is dependent on TGFβ signaling. *Development* **139,** 1921–1930
72. Shimazaki, M., Nakamura, K., Kii, I., Kashima, T., Amizuka, N., Li, M., Saito, M., Fukuda, K., Nishiyama, T., Kitajima, S., Saga, Y., Fukayama, M., Sata, M., and Kudo, A. (2008) Periostin is essential for cardiac healing after acute myocardial infarction. *J. Exp. Med.* **205,** 295–303
73. Norris, R. A., Damon, B., Mironov, V., Kasyanov, V., Ramamurthi, A., Moreno-Rodriguez, R., Trusk, T., Potts, J. D., Goodwin, R. L., Davis, J., Hoffman, S., Wen, X., Sugi, Y., Kern, C. B., Mjaatvedt, C. H., Turner, D. K., Oka, T., Conway, S. J., Molkentin, J. D., Forgacs, G., and Markwald, R. R. (2007) Periostin regulates collagen fibrillogenesis and the biomechanical properties of connective tissues. *J. Cell. Biochem.* **101,** 695–711
74. Badenhorst, D., Maseko, M., Tsotetsi, O. J., Naidoo, A., Brooksbank, R., Norton, G. R., and Woodiwiss, A. J. (2003) Cross-linking influences the impact of quantitative changes in myocardial collagen on cardiac stiffness and remodelling in hypertension in rats. *Cardiovasc. Res.* **57,** 632–641
75. Norton, G. R., Tsotetsi, J., Trifunovic, B., Hartford, C., Candy, G. P., and Woodiwiss, A. J. (1997) Myocardial stiffness is attributed to alterations in cross-linked collagen rather than total collagen or phenotypes in spontaneously hypertensive rats. *Circulation* **96,** 1991–1998